EXPLOITING THE INFRARED: IRAS OBSERVATIONS OF THE MAIN SEQUENCE

D. E. Backman and F. C. Gillett
Kitt Peak National Observatory
National Optical Astronomy Observatories††
P.O. Box 26732, Tucson, AZ 85726, USA

ABSTRACT. We examined coadded IRAS survey data on samples of nearby main sequence stars in search of far-IR excesses similar to examples attributed to clouds of orbiting grains. Of 134 systems, 25 (19%) show significant excesses at 25, 60, or 100 μm with color temperatures greater than 35 K. Approximately 15% of the stars have excess more luminous than $2 \times 10^{-5} L_{*}$, roughly independent of spectral type. Several stars with excesses appear to be older than 2×10^{9} yrs, indicating that the particle cloud phenomenon is not solely a feature of young objects.

Models of three prominent clouds that have been spatially resolved (β Pic, α PsA, and α Lyr) imply central depleted regions with radii of order 20 AU. One possible explanation for maintenance of the depleted regions is that a planet orbits at and defines each cloud's inner boundary, sweeping up particles entering that region.

The sun could have a cloud with similar geometry and somewhat smaller optical depth than these examples which would be difficult to detect from earth because of bright zodiacal and galactic emission.

1. Review of IRAS Observations of Main Sequence Stars

The IRAS mission, which lasted from January until November 1983, succeeded in surveying virtually all of the sky using a 57 cm telescope with optics cooled to < 5 K and a focal plane array of 62 detectors sensitive at 12, 25, 60, and 100 μm. Several IRAS data products are relevant to studies of main sequence stars. The Point Source Catalog (PSC) (1985) contains 250,000 sources from the survey which covered 96% of the sky. A revised catalog (PSC II) incorporates a correction for slight flux overestimation at low flux levels. A Faint Source Survey (FSS) is in progress which will coadd multiple passes in the all-sky survey, resulting in a completeness limit $\sim$3 times more sensitive than the PSC. The Low Resolution Spectra (LRS) catalog (1986) contains flux-calibrated 8-22 μm spectra with $\lambda/\Delta\lambda \sim$ 20-60 of PSC sources with $m_{12} \lesssim +4.0$. The Serendipitous Survey Catalog (SSC) (Kleinmann *et al.* 1986) lists 40,000 sources detected in 1800 AO ("Additional" or "pointed" observation) fields covering $\sim$2½% of the sky. This catalog is $\sim$5 times more sensitive than the PSC.

The statistical properties of the PSC, including detectability and characteristic far-IR properties of stars, are discussed by Chester (1985). Normal main sequence photospheres are difficult targets of study in IRAS data because: (1) The IRAS bands sample the Rayleigh-Jeans tail of Planck distributions for stellar photosphere temperatures. Thus, normal stars of all spectral types have approximately the same IRAS colors. Figure 2 in Chester (1985) is a plot of f_{25}/f_{60} vs. f_{12}/f_{25} for high galactic latitude sources

††Operated by the Association of Universities for Research in Astronomy, Inc. under contract with the National Science Foundation.

showing stars, evolved stars with circumstellar dust shells, and galaxies. The region occupied by normal stellar photospheres is small and easily distinguished. (2) The PSC includes sources at stellar temperatures only a little fainter than those detectable by the naked eye; the 12 μm completeness limit of $\sim$0.4 Jy corresponds to visual magnitude +5.0 for A dwarfs, +7.5 for G, and +10.5 for M. (3) Most stars later than spectral type mid-G detected by IRAS are giants; for example, on the basis of luminosity and space density and considering only photospheric flux, one expects to find in the PSC roughly 150 dwarfs, 5000 giants, and 30 supergiants of spectral class K. Figure 5 in Chester (1985) shows the PSC distance limit versus temperature and luminosity class; for main sequence stars later than the sun, this limit is within the distance limit of the Gliese catalog (22 pc). (4) Less than 3% of the total luminosity of objects hotter than 2000 K falls across the IRAS bands.

1.1 General Analyses of IRAS Stellar Data

Waters, Coté, and Aumann (1987) and Cohen *et al.* (1987) summarize PSC data on objects in the Bright Star Catalog (BSC) (Hoffleit and Jaschek 1982). Both papers present typical V-[12], etc. colors for a range of spectral types and luminosity classes. The authors of the first paper properly recognized that a gap at B-V $\sim$0.75 in the plot of V-[12] versus B-V between (blue) dwarfs and (red) giants is caused by the previously mentioned combination of stellar space densities and luminosities. These authors unfortunately also use an incorrect conversion from flux to magnitude that makes some of the values tabulated therein inaccurate. Some conclusions of the second paper are: (1) that median stellar colors are consistent with model atmospheres for classes O to early G, (2) Planck slopes are reasonable matches to all the observations except for cool giants, and (3) no stars have significant flux deficiencies.

Kleinmann and collaborators (priv. comm.) have selected all PSC sources above limits in galactic latitude, declination, and 12 μm flux. They have eliminated non-stellar sources on the basis of positional associations. The remaining 3000 objects are in the process of having uniform B-V colors measured from Kitt Peak. This procedure removes the color bias implicit in the previously mentioned studies, i.e., membership in both the PSC and BSC places severe constraints on V-IR color. As a result, the Kleinmann study extends to much redder stars. On the other hand, their sample excludes objects concentrated to the galactic plane which the other studies include.

1.2 Stellar Far-IR Excesses

The strong far-IR flux from α Lyrae, α Piscis Austrini, β Pictoris, and ϵ Eridani (Aumann *et al.* 1984; Gillett *et al.* 1984) is prototypical of a phenomenon which may be associated with planetary system formation. In three cases, namely β Pic, α PsA, and α Lyr, the far-IR emitting region has been resolved. The importance of spatial resolution in this context is that it has provided strong evidence that the excess emission is from particles larger than interstellar grains in orbit around the stars (Aumann *et al.* 1984, Gillett 1985).

Several searches have been conducted for more examples of stellar far-IR excesses. Aumann (1985) examined PSC data on stars with $d \lesssim 25$ pc and found that, of 36 stars detected at 12, 25 and 60 μm, 12 stars with $|b| > 10^{\circ}$ have [12]-[60] > 1.0 mag, defined there as "Vega-like". Those with excess are mostly A and F stars, and none are binaries. Sadakane and Nishida (1986) examined PSC data on BSC members and found 12 more "Vega-like" stars using criteria identical with Aumann's (1985), again mostly A-F stars, but found no deficiency of excesses in binary systems [binaries at approximately normal frequency]. Coté (1987) examined PSC data on BSC B and A stars and found 24 examples of IR excess, some of which were also noted in the previous studies. Twenty-one of these cases are defined by the author as due to dust emission, 3 to free-free emission. Jaschek, Jaschek, and Egret (1986) examined PSC data on 19 Ae / A shell stars comparable in optical spectral qualities to β Pic. They found 8 with strong far-IR excess; this is similar to the

frequency of excesses among normal A stars in volume-limited samples. There appears to be no clear correlation between optical and IR properties of the shell and emission line stars.

Section 2 of this paper presents our study of coadded IRAS survey data of volume-limited stellar samples resulting in a list of far-IR excesses similar to the prototypes in terms of color temperature and fractional luminosity (L_e/L_*). The potential detection completeness limit of our study is approximately 3 times more sensitive than studies using PSC data. Until the cases of excess listed here and in other surveys are spatially resolved and more precise IR photometry is performed, they should be considered candidates rather than definite examples of orbiting particle clouds.

Modeling results presented in §3 for the resolved systems are intended to indicate possible normal properties of the larger set of systems with excesses. The suggested connection to planetary systems is strengthened by calculation of characteristic particle sizes, cloud inner boundary radii, and particle removal time scales.

2. Investigation of Nearby Stars Using Coadded IRAS Survey Data

2.1. Sample Definition

Coaddition of the all-sky survey data yields the most sensitive photometric information available from IRAS for most of the sky. Our sample of 134 stellar systems is a subset of the Gliese Catalog (Gliese 1969; Gliese and Jahreiss 1978). The sample was limited to stars of spectral types A-K, luminosity classes V and IV-V, trigonometric parallax $\pi_t \geq 0.045$ ($d \lesssim 22$ pc), and flux ≥ 1.45 Jy in the shortest wavelength IRAS band (12 μm).

The emission from the stellar photosphere was estimated from the 12 μm flux. The flux selection criterion insured that the photospheres were determined to the same minimum accuracy. Of the prototype objects, only one (β Pic) has a significant excess at 12 μm when referred to 1-5 μm photometry (Koornneef 1983). In that case, using the 12 μm flux as the photosphere results in a slight underestimate of the excess at 60 and 100 μm.

Spectral types B and M are excluded because: (1) only 1 B and 7 M stars meet the selection criteria, and (2) far-IR excesses with fluxes similar to those studied here may also be produced around M flare stars by synchrotron emission from continuous micro-flaring (D. Mullen, priv. comm.), and around Be stars by free-free emission (e.g., Coté 1987).

Binary systems are counted as single objects, identified by the name of the primary. Stellar companions do not measurably affect net system colors at the wavelengths of IRAS sensitivity. Emission from components within radii of 23 arcsecs in-scan and 137 arcsecs cross-scan from the main component would have been included in the determination of photospheric flux at 12 μm. The summed luminosity of components listed by Gliese (1969) was used in calculating fractional cloud luminosities.

IRAS fluxes from "Addscan" processing for the final sample of stars are listed in the Appendix, Table A1. Noise-weighted mean or median scans were used. The positions in table A1 include proper motion to 1983.5 (IRAS mid-mission) and are the positions used in the processing. The fluxes are from fits to a point source template when the point source correlation coefficient and signal-to-noise ratio were high, otherwise they are peak fluxes. Upper limits are quoted for 60 and 100 μm sources which were more than 1 arcmin from the corresponding 12 μm peak position and/or did not have approximately the shape of a point source. Two objects that qualified on the basis of parallax and measured or predicted 12 μm flux are not in the final sample: Gliese 836.6AB = μ^1/μ^2 Cyg (F6/F3), which is in a region of sky not covered by the IRAS survey, and Gliese 765.0 = θ Cyg (F4), which is adjacent to a powerful 60/100 μm source.

All 134 systems were detected at 25 μm and all but 27 were detected at 60 μm. The volume searched decreases with later spectral type as a result of the 12 μm flux limit of our sample. Table I lists as a function of spectral type an estimate of the sample distance limit (reciprocal of 25th percentile π_t), the number of stars in the sample, the fraction of sample stars with significant (> 3σ) excesses, and the fraction of sample stars with significant excesses stronger than a fractional luminosity of 2×10^{-5}. The preceding statistics contain a small bias because upper limits at 60 μm were not taken into account.

TABLE I – STATISTICAL PROPERTIES OF THE SAMPLE

type	approx. limit (pc)	number	excess >3σ	excess $r \geq 2\times10^{-5}$
A	20	22	45%	23%
F	18	51	12%	12%
G	15	39	13%	10%
K	7	22	18%	18%

2.2. Measurement of Excess Flux

The amount of excess e_λ in a band was defined by:

(1) $\quad e_\lambda = [f_\lambda - f_{12}/x] \pm [\sigma_\lambda^2 + (\sigma_{12}/x)^2 + (yf_{12}/x^2)^2]^{1/2}$,

where $f_{12}\pm\sigma_{12}$ is the 12 μm flux density, $f_\lambda\pm\sigma_\lambda$ is the flux density in the band, and $x\pm y$ is the assumed photospheric flux density ratio between 12 μm and the given band. Flux uncertainties were taken to be r.m.s. dispersions about quadratic fits to the background flux density more than 2 arcmin from the source positions. An additional extrapolation uncertainty of ±3% was assumed for each band.

The photospheric flux ratios were determined from the observed 12/25 micron ratios. There are few examples of significant excess at 25 μm, so the measured 12/25 μm ratios (after removal of cases of clear excess) were assumed to represent true photosphere properties. The median 12/25 μm flux ratios (without color correction) were: spectral class A, 3.87; F, 3.93; G, 4.16; K, 4.04. These ratios were extrapolated at constant color temperature for each spectral type to determine the photospheric 12/60 μm and 12/100 μm flux ratios. The ratios used are redder than the colors assumed for bright stars in the IRAS flux calibration (Explanatory Supplement to the IRAS Catalogs, 1987). This may reflect a calibration error in the Addscan processing at that time (5/87) and/or a possibility that most main sequence stars have some far-IR excess above predictions of current model atmospheres. There are only 4 examples of flux deficiencies $\geq 3\sigma$, providing evidence that excesses $\geq 3\sigma$ are significant and that "σ" values derived from measurement uncertainty are approximately correct.

The color temperatures of the significant excesses are shown in the histogram in Figure 1. The source color temperature was calculated from the 25/100 μm flux ratio if there was 25 μm excess or from the 60/100 μm ratio if there was not. Temperatures in cases of 60 or 100 μm flux upper limits were evaluated using 3σ limits as fluxes. Figure 1 is divided into two sections: excesses more significant than 10σ, and excesses with significance between 3 and 10σ.

Many of the weaker excesses are reported here for the first time because of the sensitivity of coadded survey data. References are given in the last column of table II for stars previously recognized as having far-IR excess.

The likeliest interpretation of the cold excesses ($T \leq 35$ K) is source confusion rather than particle clouds around the stars because: (1) the objects with $T \leq 35$ K are concentrated toward the galactic plane as one would expect for "cirrus" contamination, whereas the objects with $T > 35$ K are not, (2) the warmest well-studied "cirrus" source has a color temperature

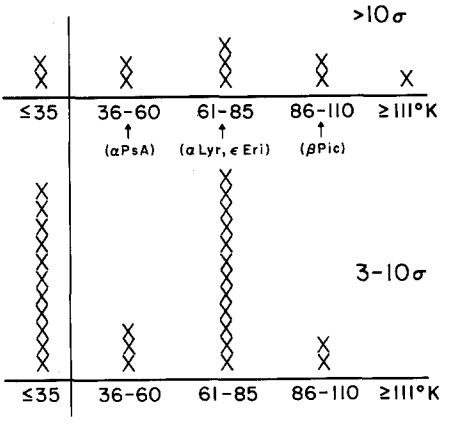

Figure 1: Color temperatures of high- and moderate-significance excesses

of 34 K (Low *et al.* 1984), and (3) the object with the highest significance in the low temperature bin is α Canis Majoris; its excess cannot be caused by solid grains warmed by the star because the required angular size would be larger than the 100 μm detector field of view (Backman, Gillett, and Low 1986). It should be noted, however, that the relative centering of α CMa and 100 μm source imply that the source is probably at the star.

The density of point sources with 35 K < $T_c \leq$ 120 K and flux > 0.10 Jy in at least one band is 11 per square degree at $|b| > 64^\circ$ and 8 per square degree at $|b| < 6^\circ$ (Kleinmann *et al.* 1986). These sources are detected most easily at 60 μm. The IRAS 60 μm FOV is 2×10^{-3} square degree. One may expect, therefore, that ~2-3 (= 134 x 2×10^{-3} x 8-11) of the 25 warm excesses around the 134 sample stars are actually due to source confusion. Similarly, the density of sources with $T_c \leq$ 35 K is 4 per sq. deg. at $|b| > 64^\circ$ and 21 per sq. deg. at $|b| < 6^\circ$. Using the 100 μm FOV and integrating over latitude, it appears that ~6 of the 13 cold excesses may be due to source confusion.

Twenty-five stars with significant far-IR excesses at 25, 60, or 100 μm comparable in temperature to β Pic, α PsA, α Lyr, and ϵ Eri are thus found in our sample of 134. These stars, their spectral types, excess flux densities (not color corrected) and associated significance, excess color temperature, and fractional cloud luminosity are listed in table II.

2.3. Frequency of Excess Versus Spectral Type

The fourth column of table I gives the frequency of excesses above 3σ significance as a function of spectral type. The previously noted large proportion of A stars with far-IR excesses is partly due to a luminosity effect (Aumann 1985; Sadakane and Nishida 1986); if the geometry and surface area of the clouds are similar from star to star, the clouds around A stars in a given volume will be most readily detected.

It is useful, therefore, to compare the excesses on the basis of a property that is independent of the stellar characteristics. An appropriate quantity is the fractional luminosity of the particle cloud, $\tau \equiv L_e/L_*$, listed in table II. This quantity equals the fraction of "sky" blocked by particles as seen from the central star. The fractional luminosity is calculated by:

$$(2) \qquad \tau = (3.1e_{25}+1.4e_{60}+0.3e_{100})\times10^{-4}/10^{[.4(4.75-m_v-B.C.)]}$$

where the e_λ are excess fluxes in Janskys. The excesses discovered so far

TABLE II – STARS WITH 25, 60 or 100 μm EXCESSES >3σ AND T > 35 K

Gliese		spec	25 μm excess (Jy)	e/σ_e	60 μm excess (Jy)	e/σ_e	100 μm excess (Jy)	e/σ_e	T_c	τ	age (Gyr)	IRAS refs
68.0	DM+19 °279	K1	0.10	1.7	0.11	3.4	0.38	2.9	85 K	7.1e-5		
71.0	τ Cet	G8	0.06	0.7	0.08	2.1	0.42	6.0	76	1.2e-5	3.5	B
111.0	τ^1 Eri	F6	0.17	3.9	0.89	35.6	3.65	22.7	62	2.2e-4	2.2±1.6	A2
121.0	τ^3 Eri	A4	0.02	0.8	0.04	1.6	0.15	3.4	75	7.5e-6		
144.0	ϵ Eri	K2	0.29	3.9	1.33	41.7	2.27	41.6	74	9.7e-5		G
167.1	γ Dor	F0	0.05	2.2	0.21	9.3	0.21	4.1	83	3.0e-5		A2
217.1	ζ Lep	A3	0.68	15.4	0.40	12.9	<0.11	- -	139	7.1e-5		C
219.0	β Pic	A5	9.05	194.1	20.44	363.4	13.15	115.3	106	2.4e-3		G
245.0	ψ^5 Aur	G0	0.11	2.6	0.43	8.9	0.53	2.4	81	1.7e-4	3.8	
248.0	α Pic	A5	0.13	3.5	0.00	0.1	<0.19	-	79	9.2e-6		
292.0A	DM–34 °4036	F5	0.03	0.9	<0.03	-	3.54	4.2	49	1.5e-4	<2.1	
297.1	B Car	F5	0.04	2.0	1.76	51.8	3.05	16.9	52	3.5e-4	4.5±1.1	
321.3A	δ Vel	A0	0.03	0.4	0.29	6.9	<0.02	-	63	2.8e-6		C
364.0	DM–23 °8646	G0	0.12	2.8	0.13	5.4	0.24	3.0	98	7.2e-5	2.6	
448.0	β Leo	A3	0.41	5.5	0.77	14.9	0.63	7.0	109	1.9e-5		A2,C
557.0	σ Boo	F2	0.06	2.2	0.09	3.5	<0.06	-	83	2.3e-5	2.0±1.5	
580.1	β Cir	A3	0.07	0.8	2.72	4.5	<9.58	-	42	1.7e-4		
584.0A	η CrB	G2	0.02	0.8	<-0.03	-	0.23	4.9	69	2.0e-5		
673.1	DM–24 °13337	A9	0.15	1.3	1.02	2.9	11.48	5.9	52	2.9e-4		
691.0	μ Ara	G5	0.22	7.3	0.08	1.1	<0.96	-	67	1.0e-4		
721.0	α Lyr	A0	1.14	3.4	7.85	114.7	8.89	48.1	74	1.5e-5		A1,G
764.0	σ Dra	K0	0.04	1.5	-0.00	-0.1	0.43	3.5	70	2.0e-5		
820.0A	61 Cyg	K5	0.38	5.1	0.57	5.0	2.38	1.9	77	1.5e-4		B
822.0A	δ Eql	F8	0.15	3.8	0.07	2.2	0.48	4.9	88	5.4e-5	6.4±1.0	
881.0	α PsA	A3	0.34	2.3	8.66	157.2	11.95	109.3	58	5.0e-5		G

References: A1 = Aumann *et al.* 1984; A2 = Aumann 1985; B = Backman, Gillett, and Low 1986; C = Coté 1987; G = Gillett *et al.* 1984

have fractional luminosity ranging from $\sim 10^{-6}$ to $\sim 10^{-3}$. In contrast, the luminosity of the known zodiacal dust emission in our (inner) solar system is $\sim 8 \times 10^{-8}$ $L_\odot$ (J. Good, priv. comm.).

The last column of table I gives the number of excesses qualified both by >3σ significance and fractional luminosity $\tau \geq 2 \times 10^{-5}$ (cf. a value of 1.5×10^{-5} for α Lyr). It appears possible that far-IR excesses occur equally often, within the uncertainties of small number statistics, in main sequence spectral classes A through K. The chosen cutoff in fractional luminosity corresponds closely to the limit of detectable excess around G and K stars in our sample but is well above the detectability limit around A stars. Increased sensitivity for the same search volumes would therefore likely increase the fraction of G and K stars found to have excesses without increasing the fraction of A stars.

2.4. Discussion

The preceding statistics lead to the conclusion that most main sequence stars have particle clouds emitting in the far-IR. The evidence for this is: (1) in cases where the illumination source is brightest, namely A stars, the proportion of stars with excesses detectable by IRAS approaches 50%; (2) stellar properties such as spectral type, rotation (v sin i), or status as a spectroscopic binary are not strongly correlated with the presence of an excess stronger than a cutoff in fractional luminosity; (3) some stars as old as the sun have detectable clouds (see below); and, (4) there is no reason to believe that the chosen cutoff in significance corresponds to a lower limit in cloud luminosities.

A particle cloud in the ecliptic plane around the perimeter of our solar system could remain undetected because, from earth's position, the diffuse surface brightness of the cold material would be masked by strong 60 and 100 μm emission from inner solar system and galactic dust. One can calculate the limit on fractional luminosity of a particle cloud around the sun such that it would not be detected from earth.

Figure 2, adapted from Good, Hauser, and Gautier (1986), shows the surface brightness of the sky in the IRAS 60 and 100 μm bandpasses as a function of ecliptic latitude. The upper set of plots indicates the observed brightness plus a smooth curve representing a model fit to the general uniform emission. The lower set of plots indicates the residuals after the model emission has been subtracted. Some of the residual is organized in "spikes" identified as dust bands produced by recent asteroid collisions (Sykes and Greenberg 1986). The strongest peak is the galactic plane.

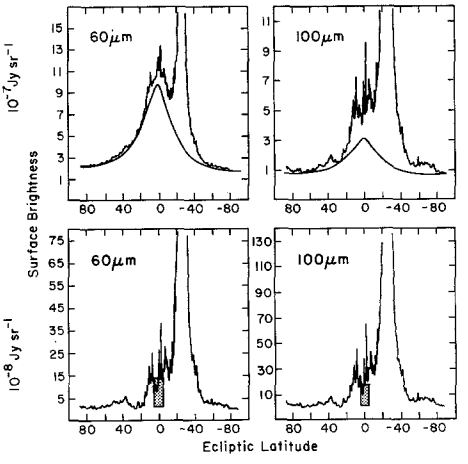

Figure 2: Observed, model, and residual zodiacal far-IR brightness compared to a hypothetical outer solar system cloud.

Superposed on the lower diagrams are markers indicating the amount of surface brightness we would observe at the earth if there were a cloud in the ecliptic plane with: (1) the same emissivity and radial extent as the α Lyr cloud (§3), (2) a fractional luminosity $\tau = 5 \times 10^{-6}$, ~1/4 the value for α Lyr, and (3) a range of inclinations $\pm 5^{\circ}$ about the ecliptic, corresponding to the thickness of the β Pic disk at r = 300 AU (Smith and Terrile 1984; Gradie *et al.* 1987).

It appears that the sun could have an undetected particle cloud beyond the outer planets having properties consistent with the clouds around nearby main sequence stars. Such a cloud might be apparent to an "outside" observer using an IRAS-type instrument but difficult for "inside" observers to discern. A cloud with greater optical depth would also be dimmer than the zodiacal and galactic emission if either its inner boundary radius or its angular size (spread of inclinations) were increased.

The last column of table II gives age estimates in units of 10^9 yrs for some of the F and and G stars with significant excess. The F star ages (Varsik 1987) are calculated from comparison of Stromgren photometry to isochrones calibrated by VandenBergh (1983). The G star ages are from emission line strengths or Li abundances calibrated by Simon, Herbig, and Boesgaard (1985) and Duncan (1981), respectively. Some stars with ages comparable to the age of the solar system apparently have particle clouds. Thus it seems unlikely that the clouds are evidence of ongoing planetary accretion.

3. Models of the Resolved Clouds

3.1. Model Procedures and Results

An important property of thermal emission from grains around stars is that the emission spectrum of each grain identifies its relative radial location in the cloud. The cloud's net emission spectrum can be translated into a range of grain temperatures. The range of orbital radii corresponding to the temperature range depends on the particles' thermal efficiency which in turn depends on the characteristic particle size. The available spatial information yields characteristic angular radii for the clouds and thus can be used to deduce particle sizes for β Pic, α PsA, and α Lyr. Results for a range of assumptions can be found in Backman *et al.* (1988). The models were fit to the observed fluxes and 60 μm scan profiles after subtraction of the contribution from the central stars.

The data used in our models are from special IRAS observations providing precise photometry and profiles sampled every 3.6 arcsecs across the sources. Ground-based 10 and 20 μm photometry of β Pic in small circular apertures was also used to constrain models of that cloud.

The particles were assumed to have: (1) absorptive/emissive efficiency $\epsilon = 1/(1+\lambda/\lambda_o)$ with parameter λ_o, smoothly varying between grey efficiency for radiation with $\lambda << \lambda_o$ and efficiency $\epsilon \propto 1/\lambda$ for $\lambda >> \lambda_o$, and (2) projected particle number in the ring between r and r+dr following a power law: $n(r)dr \propto r^{\gamma+1}dr$, with parameter γ. A value $\gamma = 0$ corresponds to a volume density distribution $\propto r^{-1}$ in a "wedge" disk (figure of rotation of an angle θ subtended at the star); this distribution and shape are consistent with the effects of Poynting-Robertson drag (see below).

Table III gives model results for the case in which γ equals 0 and λ_o has a single value. Included are: wavelength of characteristic emissivity break λ_o, inner and outer cloud radii, corresponding small-grain temperatures, total particle area, (radiative) Poynting-Robertson orbit decay time from the cloud inner radius, and stellar main sequence lifetime.

TABLE III - MODEL RESULTS FOR $\gamma = 0$, SINGLE VALUE OF λ_o

	λ_o (μm)	r_1 (AU)	T_1	r_2 (AU)	T_2	A (cm^2)	t_{PR} (yrs)	$t_{m.s.}$ (yrs)
β Pic	0.8	17	210 K	790	45 K	5×10^{30}	1×10^{4}	2×10^{9}
α PsA	80	26	115 K	450	32 K	3×10^{28}	1×10^{6}	1×10^{9}
α Lyr	1100	22	165 K	245	50 K	4×10^{27}	3×10^{6}	5×10^{8}

The value of λ_o does not imply that the particles have exactly one size, only that their thermal properties can be matched in bulk by a one-parameter model. Most of the radiating area would be contributed by the smallest particles and λ_o would characterize the minimum particle size in a steep size distribution.

If $\gamma = -1$ is used, r_1 and r_2 increase over the $\gamma = 0$ solutions by about 30%. The existence of a central region significantly depleted in particles in each case is clear, however. For example, the average density of material around α Lyr at $r < r_1$ cannot be larger than ~0.2 of its value at r_1 or there would be significantly more 12 and 25 μm flux than is observed.

3.2. Central Depleted Regions

The existence of a central depleted region in the case of β Pic was proposed by Smith and Terrile (1984) on the basis of lack of extinction on the direct line of sight to the star through the disk. They hypothesized that the region was cleared by incorporation of material into planets.

Water ice sublimation (Isobe 1970) would occur at temperatures close to 100 K. The inner radii of the α Lyr and β Pic clouds are at substantially higher temperatures and thus the depletion is not a result of ice sublimation. E. Levy (priv. comm.) has suggested that if the particles are charged, their dynamics would be determined by stellar winds, and the edges of the

central regions could represent equivalents of the heliopause. However, this mechanism would be unlikely to work for particles in the millimeter size range, as around α Lyr.

Two other particle removal mechanisms, particle-particle collisions and Poynting-Robertson (PR) drag, should be effective in these clouds and may be connected to the presence of the depleted regions. PR drag (e.g., Burns, Lamy, and Soter 1979) causes particles orbiting in a radiation field to spiral toward their force center. First-order calculations indicate that destruction of particles by mutual collisions should occur at least as rapidly as removal by PR drag. However, modest stellar winds would produce substantial additional "corpuscular" PR drag.

For the three modeled cases, the mean particle size is progressively larger for smaller total particle area. A progression in particle size versus total particle area could indicate that the identity of large particles is maintained over time and that small particles are not being replaced with fragments of larger bodies, i.e., that a PR-like effect is important. The progression in particle size is in the same sense as the stellar luminosities, so a connection to minimum stable particle size (Gillett 1985) may also be involved.

The last two columns of table III compare the stars' main sequence lifetimes (Gillett 1985) with (radiation) PR decay time for the particles at the inner edges of the clouds. A density of 3 g cm^{-3} and a particle radius related to the emissivity parameter by: $a = \lambda_o/2\pi$ were assumed. The orbital decay time for the inner particles is short compared to the stellar lifetimes.

One possible explanation for the continued existence of the depleted regions is the presence of an object able to clear a sufficiently wide volume of particles by gravitational accretion. Particles moving toward the star would be unable to cross through this volume. Matese *et al.* (1987) have also concluded that the three A star clouds have significant gaps that can be explained by the presence of planets controlling the motion of the infrared-emitting grains.

The size of the necessary large object in the case of the β Pic system can be estimated as follows. An object at $r = r_1 = 17$ AU will have orbital velocity $v_o = 9.4$ km s^{-1} and a period $P_o = 55$ yrs. A grain with $\beta \equiv F_{rad}/F_{grav} = 0.5$ will have an orbital velocity in the radiation-altered potential of:

$$(3) \qquad v_g = [(1-\beta)GM_* r^{-1}]^{1/2} = 6.6 \text{ km s}^{-1},$$

thus $\Delta v = 2.8$ km s^{-1} with respect to the large object. A black grain with $\beta = 0.5$ will have $a\rho = 3L_*/8\pi GM_* c$, where a = particle radius and ρ = particle density. The PR radial drift velocity of such a grain will be:

$$(4) \qquad v_r = GM_*(1-\beta)[(1+\beta)cr]^{-1} = 9.8 \text{ cm s}^{-1}.$$

The impact parameter "s" for gravitationally focused impact onto an object is:

$$(5) \qquad s \leq [R_o^2 + 2GM_o R_o v_\infty^{-2}]^{1/2}.$$

The time to drift across a zone of width 2s centered on the large object's orbit must be more than the relative period of the object and grain, $P_{rel} = P_o v_o/\Delta v = 185$ yrs, for capture to occur. Substituting values for Saturn, $R_o = 6.0 \times 10^9$ cm, $M_o = 5.6 \times 10^{28}$ g, and equating v_∞ to Δv, one gets $2s = 4.9 \times 10^{10}$ cm, which would be crossed by the grain in 170 yrs. A product of mass and radius slightly larger than Saturn's would thus be the minimum necessary to limit the β Pic cloud.

Acknowledgments: The authors would like to thank G. Neugebauer, F. Low, and H. Aumann for assistance with the IRAS slow-scan observations and reductions, S. Aoki for assistance with the Addscan reductions, M. Cook and J. DuHamel for preparation of the figures, I. Gatley, E. Becklin, J. Goad, and S. Kleinmann for helpful discussions, the Data Management Team of IPAC, especially H. Hanson, for rapid production of the Addscan data, and the IPAC library chopper crew for heroic bundling and mailing.

REFERENCES

Aumann, H. H., Gillett, F. C., Beichman, C. A., de Jong, T., Houck, J. R., Low, F. J., Neugebauer, G., Walker, R. G., and Wesselius, P. R. 1984, Ap. J. Lett. **278**, L23.
Aumann, H. H. 1985, P. A. S. Pacific **97**, 885.
Backman, D. E., Gillett, F. C., Aumann, H. H., Neugebauer, G., Low, F. J., and Waters, R. 1988, in prep.
Backman, D. E., Gillett, F. C., and Low, F. J. 1986, Adv. in Space Res. **6** (7), 43.
Burns, J., Lamy, P. L., and Soter, S. 1979, Icarus **40**, 1.
Chester, T. J. 1985, in Light on Dark Matter, ed. F. P. Israel, Reidel Co., Dordrecht, p. 3.
Cohen, M., Schwartz, D. E., Chokshi, A., and Walker, R. G. 1987, A. J. **93**, 1199.
Coté, J. 1987, A. A. **181**, 77.
Duncan, D. K. 1981, Ap. J. **248**, 651.
Explanatory Supplement to the IRAS Catalogs and Atlases 1987, eds. C. A. Beichman, G. Neugebauer, H. J. Habing, P. E. Clegg, and T. J. Chester (US Government Printing Office).
Gillett, F. C., Aumann, H. H., Low, F. J., Neugebauer, G., Waters, R. 1984, paper presented at Protostars and Planets II Conf., Tucson.
Gillett, F. C. 1985, in Light on Dark Matter, ed. F. P. Israel, Reidel Co., Dordrecht, p. 61.
Gliese, W. 1969, Catalogue of Nearby Stars , Veröffentl. Astron. Rechen-Instituts, Heidelberg, Nr. 22.
Gliese, W. and Jahreiss, H. 1979, A. A. Suppl. **38**, 423.
Good, J. C., Hauser, M. G., and Gautier, T. N. 1986, Adv. in Space Res. **6** (7), 83.
Gradie, J., Hayashi, J., Zuckerman, B., Epps, H., and Howell, R. 1987, paper presented at Lunar and Planetary Science Conf. XVIII, Houston.
Hoffleit, D., and Jaschek, C. 1982, The Bright Star Catalog, 4th revised ed., Yale University Observatory, New Haven.
IRAS Catalogues and Atlases: Atlas of Low Resolution Spectra, F. M. Olnon and E. Raimond, eds., 1986, A. A. Suppl. **65**, 607.
IRAS Point Source Catalog 1985, Joint IRAS Science Working Group (US Government Printing Office).
Isobe, S. 1970, P. A. S. Japan **22**, 429.
Jaschek, M., Jaschek, C., and Egret, D. 1986, A. A. **158**, 325.
Kleinmann, S. G., Cutri, R. M., Young, E. T., Low, F. J., Gillett, F. C. 1986, IRAS Serendipitous Survey Catalog (US Government Printing Office).
Koornneef, J. 1983, A. A. Suppl. **51**, 489.
Matese, J. L., Whitmire, D. P., Lafleur, L. D., Reynolds, R. T., and Cassen, P.M. 1987, AAS Division of Planetary Sciences Conf., abstract.
Low, F. J., *et al.* 1984, Ap. J. Lett. **278**, L19.
Sadakane, K. and Nishida, M. 1986, P. A. S. Pacific **98**, 685.
Simon, T., Herbig, G., and Boesgaard, A. M. 1985, Ap. J. **293**, 551.
Smith, B. A. and Terrile, R. J. 1984, Science **226**, 1421.
Sykes, M. V. and Greenberg, R. 1986, Icarus **65**, 51.
VandenBergh, D. A. 1983, Ap. J. Suppl. **51**, 29.
Varsik, J. 1987, Ap. J. (preprint).
Waters, L. B. F. M., Coté, J., and Aumann, H. H. 1987, A. A. **172**, 225.

Discussion following talk by **Backman**:

Deming: The zodiacal light was a significant source of background for IRAS. This suggests that with improved spatial resolution, solar-type zodiacal clouds might be detectable around nearby stars. Will SIRTF be able to do this?
Backman: SIRTF's expected broadband sensitivity at 25 μm is $\sim 2 \times 10^{-5}$ Jy (1σ, 900 sec). Our solar system's zodiacal dust would yield $\sim 4 \times 10^{-4}$ Jy contained in a diameter of < 1 arcsec if viewed from a distance of 8 pc (α Lyr), hence detectable in principle but not resolvable by SIRTF. However, the flux from the Sun itself would be 0.5 Jy, so one would need to be able to predict the photospheric flux to better than 1 part in 10^3 in order to realize there was an excess caused by dust.
Stencel: Do you have any thought about the origin of the IR excesses in general and in the context of LeeAnne Willson's speculation about pulsation-driven mass loss evolving young A type dwarfs, down the main sequence?
Backman: The present mass loss from α Lyr and α PsA is known from UV spectra and radio upper limits (e.g. Hollis et al., Ap. J., 294, 646 (1985)) to be orders of magnitude less than the amount required to carry the mass of observed grains. A wind as slow as 1 km s^{-1} would cross the radial extent of the clouds in < 100 yrs, so one would have to suppose we are fortuitously observing 3 recently extinguished winds. On the other hand, strong stellar winds might tend to accelerate the collapse of the clouds by Poynting-Robertson drag.
Linsky: Please comment on whether the spatially resolved 60 micron excess emission seen around β Pic and other stars could be produced by clouds of comets similar to the Oort cloud of comets predicted to exist around the Sun.
Backman: Oort cloud comets are supposed to be former Uranus/Neptune-Zone planetesimals tossed by encounters with the protoplanets into orbits with large aphelia. Subsequent perturbation by passing stars produced the present spherical system with perihelia detached from (i.e. beyond) the planetary region. The "classical" Oort cloud lies at radii $> 20{,}000$ AU, although there could be substantial numbers of comets closer than that. There is not a strong resemblance to the m.s. particle clouds with r < 1000 AU, probably organized as disks. However, a comet belt, relic of the pre-solar disk could extend in the ecliptic plane beyond Neptune. Such a system would more closely resemble what we see at β Pic. The small particles might be "chips" of larger comet parent bodies invisible to IRAS (Weissmann, Science, 224, 987 (1984), Harper et al., Ap. J., 285, 808 (1984)).
Strom: To what distance/mass limit can β Pic-like structures be detected?
Backman: β Pic far-IR excess could be detected in IRAS data to a distance of 150 pc in coadded survey data, 200 pc in pointed observations. This is the m.s. cloud with the highest known fractional luminosity ($2 \times 10^{-3} L_*$. A number of T Tauris are close enough to be checked. However, detection near the distance limit would involve noting a weak 25/60 μm source at the same position (to arcmin accuracy) as an $\sim$8th mag star, so one would not necessarily be confident of a connection between star and far-IR source, especially in crowded fields/near the galactic plane where T Tauris tend to live.